Applied Catalysis B: Environmental 84 (2008) 196–203

Contents lists available at ScienceDirect

Applied Catalysis B: Environmental

journal homepage: www.elsevier.com/locate/apcatb

Characterization and enhancement of carbon nanotube-supported PtRu electrocatalyst for direct methanol fuel cell applications

Ning-Yih Hsu, Chun-Ching Chien, King-Tsai Jeng *

Institute of Nuclear Energy Research (INER), P.O. Box 3-19, 1000 Wenhua Road, Longtan, Taoyuan 32546, Taiwan

ARTICLE INFO

Article history:
Received 27 September 2007
Received in revised form 25 March 2008
Accepted 25 March 2008
Available online 8 April 2008

Keywords:
Direct methanol fuel cell
Carbon nanotube
Electrocatalyst
Catalyst oxidation states
CO stripping
Activation time

ABSTRACT

In this study, a carbon nanotube-supported PtRu electrocatalyst (PtRuCNT) was prepared, characterized and investigated for methanol electro-oxidation by catalytic activity enhancement using an electrochemical treatment. From XPS analyses, the as-prepared catalyst was found to mainly composed of Pt(0)/Pt(II) states for the Pt element and Ru(0)/Ru(IV) states for the Ru element. When the electrocatalyst was subjected to an enhancement treatment, the Ru(IV) state increased substantially from 29.50% to 44.11%. Both CO-stripping experiments and open-circuit cell voltage measurements indicated that the treated PtRuCNT has given rise to an improved performance on methanol electro-oxidation caused mainly by the increase of the Ru(IV) state in this particular case. The single-cell test also revealed that a direct methanol fuel cell (DMFC) can be put into its full operation in a short time. A direct application of this finding is to significantly shorten the activation time of a new DMFC stack. However, the electrochemically treated PtRuCNT catalyst still needs a continuous enhancement mechanism to sustain its enhanced activity. A promotional model is proposed to explain the phenomenon observed and a remedial approach is also suggested to solve the problem for practical applications.

1. Introduction

Direct methanol fuel cells (DMFCs) have several advantages over other types of fuel cell to be used as dependable and long-lasting portable power sources to replace batteries in a variety of electronic products, including laptop computers and cellular phones. Although significant advances have been achieved for the DMFC systems in recent years, considerable efforts are still needed to put them into real commercialization with smaller sizes, lower costs and better durability. In addition to a variety of nanocatalysts currently being developed, the choice of suitable carbon support materials for the electrocatalysts is also an important factor that can significantly affect the performances of supported electrocatalysts owing to interactions, which modify the catalytic activities, between metal catalysts and carbon support materials [1]. Conductive carbon black powders, such as Vulcans, are commonly used as membrane fuel cell catalyst support materials. However, these conventional carbon materials have been investigated for a long time and substantial information has already been accumulated.

With the advancement of nanotechnology, currently the development of DMFCs has stressed on the applications of nanomaterials to the syntheses of state-of-the-art nanocatalysts. The use of carbon-based nanomaterials [2–11], e.g., carbon nanotubes, carbon nanofibers, carbon nanocoils, and carbon nanohorns, as a new generation of catalyst supports is the most common practice. This is due to the distinctive characteristics of such new carbon nanomaterials [12,13], such as more crystalline structures with high electrical conductivities, excellent corrosion resistances, and high purities containing less catalyst poisons, compared to conventional carbon black powders. The fabricated electrode is also more favorable for the transfer of reactants in the catalyst layer leading to improved fuel cell reactions. In general, the prepared catalysts were well-controlled within a suitable nanosize range. Various synthesis methods are used to prepare the catalysts with the treatment of carbon nanometarials. Such treatment uses strong acids to form surface functional groups as a prerequisite.

Since the pioneering work of Bockris and Wroblowa [14], it has been realized that the capability of PtRu electrocatalyst to exhibit a high methanol electro-oxidation activity is due to the ability of the Ru element to form active hydroxyl species with water at a low potential range, which provides the needed oxygen to CO_{ad} for the formation of CO_2 as a complete methanol electrochemical oxidation reaction. This has solved most of the catalyst-poisoning problems for the DMFC anode. At present, PtRu is the most used

* Corresponding author. Tel.: +886 3 471 1400x5310; fax: +886 3 471 3940.
E-mail address: ktjeng@iner.gov.tw (K.-T. Jeng).

0926-3373/$ – see front matter © 2008 Elsevier B.V. All rights reserved.
doi:10.1016/j.apcatb.2008.03.018

anode catalyst in a DMFC. Although a variety of modified multi-component catalysts [15–21], such as PtRuIr, PtRuP, PtRuWC, PtRuCo, PtRuRhNi, and PtRuSnW, as well as some interesting alternative catalysts [22,23], e.g., $PtCeO_2$ and PtVO, have been proposed and actively investigated, their long-term performances are still waited to be seen. However, the PtRu anode catalyst is, in fact, not a true panacea for the DMFCs as it was thought to be. Studies have shown that there are still some serious problems with this binary anode catalyst. For instance, there is a ruthenium dissolution and crossover problem [24,25], an activity–decay problem, i.e., the durability issue, and a need to significantly increase the electrocatalytic activity of PtRu for more practical applications.

It was reported [26,27] that the oxidation states of the PtRu catalyst elements play important roles in the process of methanol electro-oxidation, although the conclusions can be very conflicting caused by the pretreatment of the catalysts. It was also found [28–30] that the X-ray photoelectron spectroscopy (XPS) has provided a useful tool to the investigation of oxidation states of catalyst elements. In this study, we focused on attempting to improve the activity of the PtRuCNT anode catalyst using a simple electrochemical approach. The main idea was to convert the catalyst elements to their higher oxidation states, so it would enhance the catalytic reactions of the anode reactant on the catalyst surfaces. This is deemed to be very useful for significant improvement in the performance of a DMFC.

2. Experimental

2.1. Preparation and characterization of PtRuCNT catalyst

Multi-walled carbon nanotubes were obtained from Advance Nanopower Inc., Taiwan having diameters of 8–15 nm and an average surface area of 233 $m^2\,g^{-1}$. The length of the carbon nanotubes was found to be 1–2 μm. The as-received carbon nanotubes were first oxidized in a hot solution, composed of 8 M HNO_3 and 2 M H_2SO_4, for several hours under refluxing conditions to remove impurities and generate surface functional groups. Purification of CNT surfaces prevents self-poisoning by foreign impurities while functional group generation enhances electrocatalyst formation.

A high-metal-content PtRu catalyst, i.e., 40 wt%Pt-20 wt%Ru catalyst, supported on a multiwalled CNT material was prepared in-house using a modified polyol method as described in our previous reports [31,32]. Briefly, a known amount (0.40 g) of acid-oxidized CNT was added to 50 ml ethylene glycol (EG) aqueous solution. The above mixture was sonicated for 10 min, followed by high-speed stirring for 30 min, using a high-speed stirrer (Heidolph, Silent Crusher M) to form a homogeneous paste so that EG was able to completely cover the carbon nanotube surfaces. Then, 1.08 g of $H_2PtCl_6{}^{\bullet}6H_2O$ and 0.42 g of $RuCl_3$ used as PtRu electrocatalyst precursors were dissolved in 10 ml EG, together with addition of 1 ml of 1 M $NaHSO_3$ aqueous solution as a modifier, forming complexed salts or ions. After that, the catalyst precursor salt/EG/$NaHSO_3$ solution was slowly added to the prepared CNT/EG paste and the pH was adjusted to about 4 by dispensing a suitable amount of 4 N NaOH using a metering pump into the above mixture. The solution was subjected to high-speed stirring for the complexed metal salts or ions to adhere to the surfaces of carbon nanotubes. In the meantime, the resultant mixture was heated at 130 °C using a microwave heater for 60 min to form PtRu/CNT with the pH monitored. An inductively coupled plasma-optical emission spectroscope (ICP-OES) (Jobin Yvon, Ultima-2) was used to accurately determine the final composition of the prepared catalyst.

Physical characterization of the prepared PtRuCNT electrocatlyst was carried out using a transmission electron microscope (TEM) (JEOL, JEM 2010 operating at 200 kV) for morphology and particle-size analyses. X-ray diffraction (XRD) spectroscopy was employed to examine the formation of PtRu on the multiwalled CNT surfaces. A Siemens Diffractometer (D 5000) was used to record the patterns. Scans were acquired with a 0.02° step size over 2θ range of 20°–90°. Diffraction peaks of crystalline phase were compared with those of standard species reported in the JCPDS Data File. A scanning electron microscope (SEM) (JEOL, JSM-T330A operating at 8 kV) coupled with an energy dispersive X-ray (EDX) spectroscope was further employed for the elemental identification of the prepared catalyst.

2.2. Electrochemical enhancement, CO-stripping voltammograms and XPS characterization of PtRuCNT catalyst

A simple electrochemical enhancement approach was employed to alter the oxidation states of the catalyst elements. The prepared PtRuCNT catalyst was well-mixed in a 1 N $HClO_4$ aqueous solution containing a small amount of isopropanol as a wetting agent. The catalyst was put in the anodic compartment of a proton exchange membrane (PEM)-divided electrochemical cell. The cathodic compartment was filled with a pure 1N $HClO_4$ solution. A direct voltage of 1.1 V was applied to the electrochemical cell and the anodic compartment was continuously bubbled with nitrogen for one hour. The treated PtRuCNT catalyst was then thoroughly rinsed with deionized water and dried in an oven.

The CO-stripping voltammograms were taken using a three-electrode cell in 0.5 M H_2SO_4 solution. At the beginning, a pure nitrogen gas was purged into 0.5 M H_2SO_4 solution for 30 min and the background was recorded. Afterwards, a nitrogen gas containing 1% CO was bubbled into 0.5 M H_2SO_4 solution for 30 min. The dissolved CO in the solution was then removed by bubbling pure nitrogen gas into the solution for another 30 min. Finally, the CO-stripping voltammograms were collected between 50 and 850 mV (vs. NHE) with a scan rate of 50 mV s^{-1} under N_2. The XPS experiments were conducted using a Physical Electronics PHI 5600 multi-technique system equipped with an Al monochromatic X-ray at a power of 350 W.

2.3. Investigation on methanol electro-oxidation and performance tests of single-cell DMFC

Both the as-prepared and treated PtRuCNT catalysts were fabricated separately into electrodes by coating onto carbon cloth substrates of the same material using a suitable amount of Nafion® ionomer for each. The catalyst loading was 4 mg PtRu cm^{-2}. Briefly, a known amount of electrocatalyst was first well-mixed with a designated amount of Nafion® solution (containing 10 wt% Nafion® ionomer), together with suitable amounts of isopropanol and deionized water, and then applied to one side of a Teflon-treated carbon cloth (ElectroChem, Inc., model: EC-CC1-060T) by vacuum filtration followed by a physical leveling procedure [33]. Thereafter, the electrode was dried in air for several days before being hot-pressed into electrode and membrane assembly (MEA).

Electrochemical investigation with respect to methanol electro-oxidation was carried out by means of cyclic voltammetry. A three-electrode system was employed with Pt as the counter electrode and Ag/AgCl as the reference. The methanol electro-oxidation experiments were performed at room temperature in a 0.5 M H_2SO_4 aqueous solution containing 1 M CH_3OH with a cyclic sweep rate of 10 mV s^{-1}. A background comparison experiment was also conducted without the addition of CH_3OH in the solution.

For the single-cell DMFC performance tests, a gas diffusion electrode (GDE) with a platinum black loading of 4 mg cm^{-2}, obtained from E-TEK, was employed as the cathode. The geometric area of the electrode was 25 cm^2. In the preparation of MEA, the prepared anode and the GDE cathode were hot-pressed onto a Nafion® 117 membrane at 130 °C with an applied pressure of 0.5 kN cm^{-2} for 5 min. Then, the MEA was fabricated into a single-cell DMFC using two graphite endplates and fasten with bolts and nuts. The single-cell DMFC was first activated and the open-circuit cell voltage was measured without applying any loaded current. It was then tested at 60 °C by feeding a 1 M methanol solution (40 ml min^{-1}) through the anode compartment, and by flowing oxygen through the cathode compartment with a stoichiometric ratio of 3. The performance tests of the DMFC were conducted using a fuel cell test station developed by APFCT Inc., Taiwan. The cell performance curves, i.e., plots of cell voltage vs. current density and power density vs. current density, were collected.

3. Results and discussion

3.1. Physical characteristics of prepared PtRuCNT

It was found from the ICP-OES test that the metal deposition efficiency for the PtRuCNT catalyst was >98.52% using the modified polyol method. The prepared PtRuCNT was calculated to have an exact percentage composition of 39.27 wt%Pt-19.62 wt%Ru, which is very close to the desired atomic ratio of Pt:Ru = 50:50. This exemplified the usefulness of the modified polyol method in the preparation of the PtRuCNT catalyst to obtain a controlled catalyst atomic ratio composition. The key to success depends mainly on the creation of a suitable deposition environment on the CNT surfaces near the isoelectric point (IEP), i.e., the polarity of zeta (ζ) potential turns from negative to positive or vice versa, where both complexed platinum and ruthenium ions have almost equal specific adsorption rates. Thus, at this particular point, the composition of formed PtRu catalyst can be controlled by the composition of metal ions in the deposition solution. In general, the use of a high-metal-content catalyst is favorable for the fabrication of a DMFC electrode with a thin catalyst layer. An immediate benefit is a substantial reduction of resistance in the electrode.

The TEM image of the as-prepared PtRuCNT catalyst is shown in Fig. 1(a). One can clearly see that the prepared PtRuCNT has very uniform particle dispersion and size distribution. The particle sizes are about 2–5 nm. This has been reported [34] to be just about the ideal size of the PtRu catalyst for the methanol electro-oxidation. Fig. 1(b) illustrates the XRD pattern of the as-prepared PtRuCNT electrocatalyst. These diffraction peaks correspond to Pt(1 1 1), Pt(2 0 0), Pt(2 2 0), and Pt (3 1 1) of the Pt-rich fcc phases. However, the resultant characteristic peaks are not sharp, which indicates a somewhat amorphous structure for the catalyst. In fact, no apparent peaks corresponding to the hcp phases of the Ru element can be seen. This phenomenon is commonly found for carbon-supported PtRu electrocatalysts [35,36] except those of the highly Ru-rich particles. It can be attributed to the coincidence that the signal peaks of both Pt and Ru elements appear at almost the same positions. The Pt element has a much larger size. Therefore, it exhibits a more pronounced signal pattern than that of the Ru counterpart.

It has been observed in one of our previous studies [37] that the characteristic diffraction peaks corresponding to RuO_2(1 1 0), RuO_2(1 0 1) and RuO_2(2 1 1) will appear due to the formation of different crystalline structures. This can be achieved by oxidizing the PtRu catalyst in an oxygen environment at an elevated temperature of about 400 °C. This can be used as a complementary means to identify the presence of the Ru element in the catalyst. However, it should be noted that using heat treatment to a crystalline alloy catalyst would result in the decrease of catalyst activity for methanol electro-oxidation, probably due to a substantial decrease in the catalyst surface.

In fact, identification of the presence of Ru element in a PtRuCNT catalyst can also be resorted to the use of an EDX spectrum as shown in Fig. 1(c). It can be seen that the signal of the ruthenium element is clearly visible which is different from that of a XRD pattern. The atomic ratio of the two metals can also be roughly estimated from the relative intensity of the signal peaks. In addition, the XPS spectra are also able to provide direct evidences on the formation of the PtRuCNT catalyst.

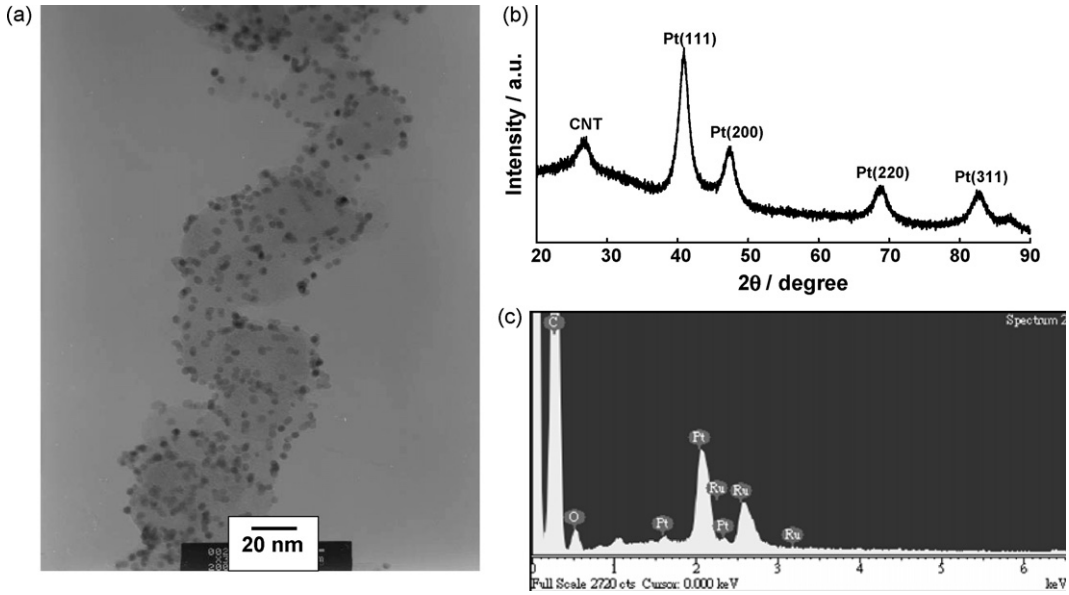

Fig. 1. (a) TEM image of as-prepared PtRuCNT catalyst indicating excellent catalyst morphology, (b) XRD pattern of as-prepared PtRuCNT catalyst, and (c) EDX spectrum of as-prepared of PtRuCNT catalyst revealing signals of the Ru element.

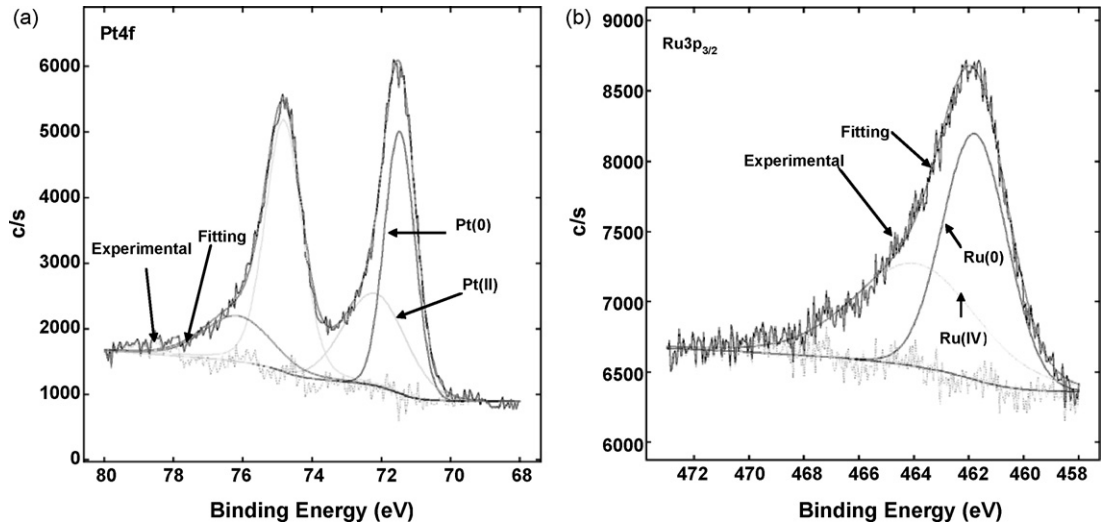

Fig. 2. XPS spectra of as-prepared PtRuCNT: (a) Pt4f and (b) $Ru3p_{3/2}$.

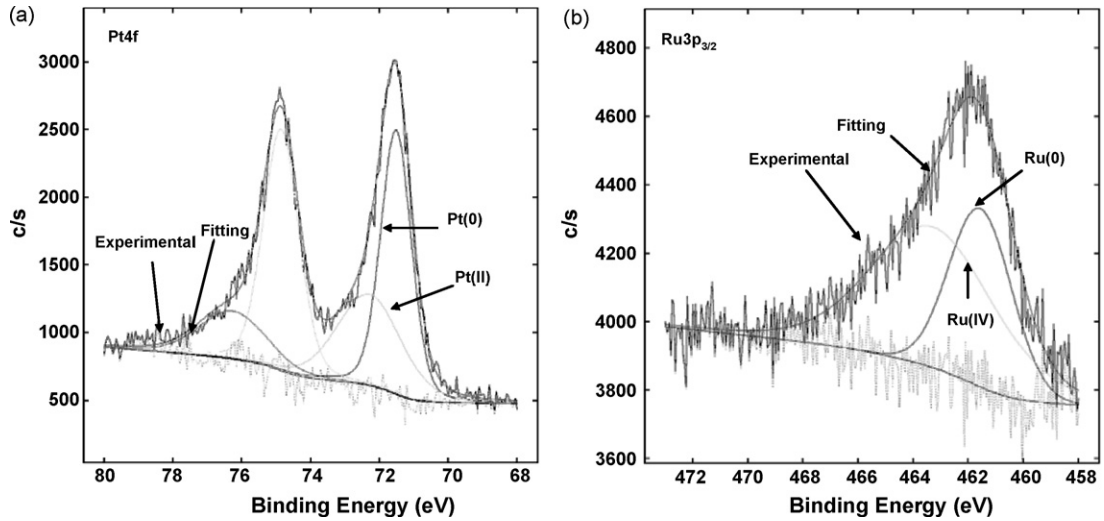

Fig. 3. XPS spectra of electrochemically treated PtRuCNT: (a) Pt4f and (b) $Ru3p_{3/2}$.

3.2. XPS characteristics of PtRuCNT with and without electrochemical enhancement

The XPS spectra for Pt4f and $Ru3p_{3/2}$ core-level regions of the as-prepared PtRuCNT are shown in Fig. 2, while those spectra for the electrochemically treated PtRuCNT are shown in Fig. 3. Due to severe interferences caused by the overlapping of the Ru3d and C1s regions, the less-intense Ru3p region was analyzed. Deconvolution of the Pt4f region shows the presence of two pairs of doublets. The more intense doublet peaks with binding energies of 71.3 eV ($Pt4f_{7/2}$) and 74.6 eV ($Pt4f_{5/2}$) are attributed to the metallic Pt. On the other hand, the peaks corresponding to 72.2 and 76.4 eV can be assigned to the Pt(II) species in a form of $Pt(OH)_2$ instead of PtO. It should be noted that the Pt(IV), or the PtO_2, species was also reported to exist in a small quantity [29]. Apparently, different methods used in the preparation of catalysts might result in different compositions of the oxidation states in the catalyst metals. The assignment of $Pt(OH)_2$ as the Pt surface species was conducted in accordance with the Pourbaix diagram [38] (i.e., the *V* vs. pH plot) of the Pt-H_2O system as shown in Fig. 4(a). After having subjected to the electrochemical enhancement treatment, the XPS spectra of the Pt element did not exhibit apparent changes. From Table 1, it can be seen that the amount of the Pt(II) species before and after having been subjected to the electrochemical enhancement treatment are 26.09% and 25.67%, respectively. These are calculated from the relative peak intensities of the

Table 1
Comparison of the PtRuCNT electrocatalysts before and after being subjected to an electrochemical enhancement treatment

PtRuCNT	Oxidation State				Bulk composition	Surface composition	EAS ($cm^2\ g^{-1}$)
	Pt(0) (%)	Pt(II) (%)	Ru(0) (%)	Ru(IV) (%)	Pt:Ru	Pt:Ru	
As-prepared	73.91	26.09	70.50	29.50	51:49	56:44	267.0
Treated	74.33	25.67	55.89	44.11	51:49	55:45	281.3
Treated after use	72.59	27.41	70.07	29.93	–	–	–

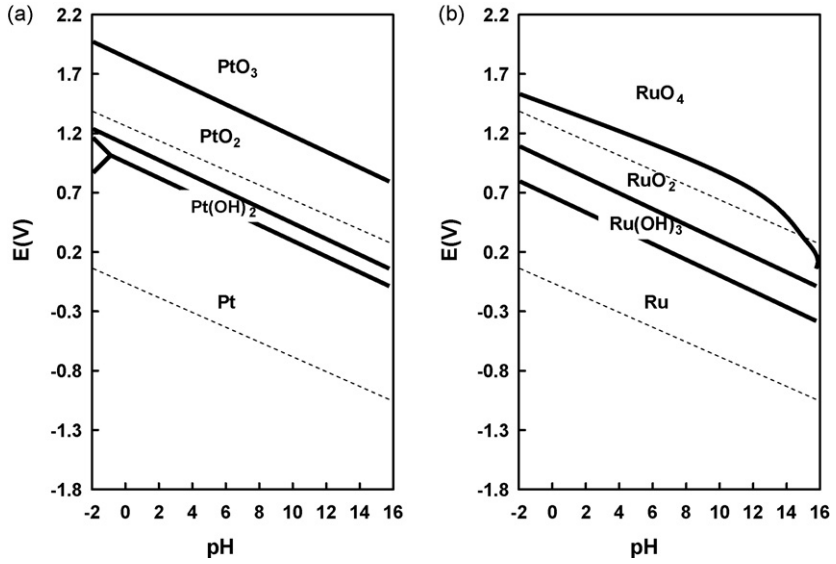

Fig. 4. Pourbaix diagrams of (a) Pt–H_2O and (b) Ru–H_2O systems.

spectra. Virtually no change in the oxidation states of the Pt element was found.

Similarly, the $Ru3p_{3/2}$ spectrum was deconvoluted into two peaks at 461.7 and 463.9 eV corresponding to the metallic Ru and the RuO_2 species, i.e., Ru(0) and Ru(IV), respectively. The assignment of the RuO_2 species was also performed in accordance with the Pourbaix diagram as illustrated in Fig. 4(b). The amount of the Ru(IV) species before and after having been subjected to the electrochemical enhancement treatment was 29.50 and 44.11%, respectively. Different from that of the Pt element, a substantial change in the oxidation states of the Ru element was found. It can be attributed to the more facile oxidation of the Ru element on its surface than that of the Pt counterpart.

After having subjected to methanol oxidation for a period of time, the XPS spectra of the treated PtRuCNT catalyst were observed to exhibit some changes as illustrated in Fig. 5. As expected, the oxidation states of the Ru element were found to turn back to almost the same as those of the as-prepared counterpart, while those of the Pt element still remained almost unchanged. The compositions of both elements were calculated and shown in Table 1. Apparently, during the electrochemical enhancement stage, the applied voltage was mostly employed to promote the formation of ruthenium oxide in this particular case. This enhanced oxide formation was significantly involved in methanol oxidation. An alternative approach to generate the higher oxidation states of the catalyst is the use of strong oxidants, such as $KMnO_4$ and O_3, to promote the oxidation of the catalyst surfaces.

3.3. Enhancement of methanol electro-oxidation and performance of single-cell DMFC

In Fig. 6, curve (a) represents the background voltammogram taken with as-prepared PtRuCNT without the adsorption of CO on the catalyst surface; it is monotonous and featureless. On the other hand, curves (b) and (c) are CO-stripping voltammograms for as-prepared and treated PtRuCNT, respectively. The peaks in the neighborhood of 390–680 mV(NHE) correspond to CO oxidation (stripping) signals. It can be seen that the CO-stripping voltammograms for these two catalysts are quite different and the onset potentials are clearly distinguishable. The onset potential for CO

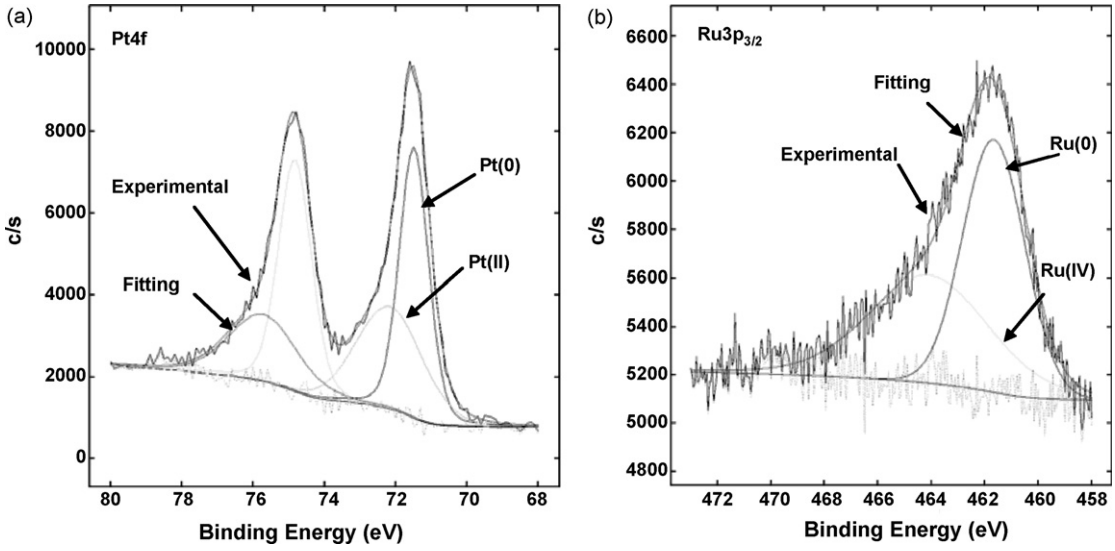

Fig. 5. XPS spectra of electrochemically treated PtRuCNT after having subjected to methanol oxidation: (a) Pt4f and (b) $Ru3p_{3/2}$.

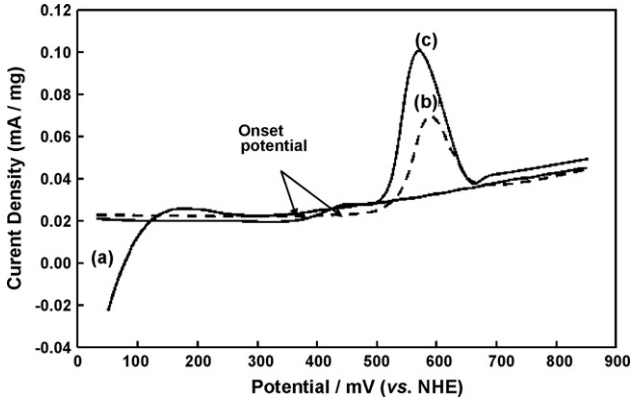

Fig. 6. CO-stripping voltammograms of (a) background (b) as-prepared and (c) treated PtRuCNT in 0.5 M H_2SO_4 at room temperature with a sweep rate of 50 mV s^{-1}.

oxidation of the later appears at a much lower value with a difference of about 100 mV from that of the former. This, in turn, causes a substantially larger CO oxidation signal. Such a phenomenon is consistent with the behavior of a more reactive catalyst species indicating that the enhancement of methanol oxidation is caused mainly by the promotion of the catalyst oxidation state.

In addition, based on the ICP analysis, the bulk composition in terms of atomic ratio of the as-prepared PtRuCNT was found to be Pt:Ru = 51:49 while that of the treated one was also Pt:Ru = 51:49. No apparent difference was observed. Similarly, from the XPS quantitative analysis, the surface composition of the as-prepared PtRuCNT was found to be Pt:Ru = 56:44 while that of the treated one was Pt:Ru = 55:45. This suggests that, unlike subjecting to activation by continuous voltammetric cycling, the one-step enhancement approach employed in this study did not cause much change in the compositions of both bulk catalysts and catalyst surfaces. Nevertheless, both catalysts were within the range of a well-mixed PtRu solid solution close to the ideal composition of 50:50 indicating that there were enough Pt and Ru elements on the catalyst surfaces to make good methanol oxidation.

However, even with the same surface composition, the surfaces of two PtRu catalysts are not ensured to be equally active. In a recent report by Hyun et al. [39], it was found that two PtRu/C catalysts with the same surface composition of Pt:Ru = 59:41 and the same particle size of 2.0 nm, the one with more Pt element at high oxidation states exhibited a much better performance in a DMFC. Also, the oxidation state of Ni was reported [40] to play a key role on the catalytic performance of PtRuNi/C electrocatalysts particularly in the CO oxidation reaction. These results indicated that the oxidation state of an electrocatalyst element can be an important factor in the methanol electro-oxidation process. In this study, the oxidation state change was found to occur mainly in the Ru element of PtRuCNT.

In the CO-stripping experiments, 10.02 mg of as-prepared and 10.01 mg of treated PtRuCNT catalyst was used, respectively. The as-prepared PtRuCNT gave a total charge of 1.4560C while that of the treated PtRuCNT accounted for 1.7044C. Thus, the performance of the later was improved by about 17.2% based on the total charge increase. If Ru(IV), in the form of RuO_2, can provide two oxygen atoms while Ru(0), by first converting to Ru-OH as an intermediate with H_2O, can provide only one oxygen atom to the overall CO electro-oxidation, then the contribution of Ru(IV) is twice that of Ru(0) in the CO stripping to form CO_2. Assuming that only Ru(0) is involved in the CO-stripping reaction, the theoretical electrochemical active surface area (EAS) of the as-prepared catalyst is calculated to be 1.4560C/420 μC cm^{-2}/10.02 mg = 345.9 cm^2 mg^{-1}. However, both Ru(0) and Ru(IV) can participate in the reaction. Taking into account the composition of oxidation states of the as-prepared catalyst, the real EAS is found to be 345.9 cm^2 mg^{-1} × 100/(70.5 + 29.5 × 2) = 267.0 cm^2 mg^{-1}. Similarly, the theoretical EAS for the treated PtRuCNT catalyst is calculated to be 405.4 cm^2 mg^{-1}. The real EAS is then adjusted to be (405.4 cm^2 mg^{-1} × 100)/((55.89 + 44.11)2) = 281.3 cm^2 mg^{-1}. Therefore, the ratio of real ESA for treated PtRuCNT to as-prepared PtRuCNT is 281.3/267.0 = 1.054. This means the contribution from EAS increase of the treated catalyst only accounts for 5.4%. Thus, our results prove that in this particular case the key factor for the enhanced catalyst activity on methanol oxidation is the oxidation state change of the Ru element in the treated catalyst rather than the EAS increase.

From the cyclic voltammograms of the as-prepared and treated PtRuCNT catalysts in 0.5 M H_2SO_4 solution as shown in Fig. 7(a), it can be seen that the current of the later is much larger indicating the formation of a substantial amount of surface oxides. This corresponds to the presence of the Ru(IV) state in a higher percentage. Similarly, in a 0.5 M H_2SO_4 + 1 M CH_3OH solution, the CV of the later as demonstrated in Fig. 7(b) also exhibits a more pronounced current signal, which clearly indicates a more catalytic surface of the treated catalyst toward methanol electro-oxidation. Both current densities for methanol electro-oxidation were expressed in terms of a unit weight and a unit area of EAS of the PtRu catalyst used. The Pourbaix diagram as illustrated in Fig. 4(b) indicates that the higher oxidation states of the Ru element is thermodynamically more favorable for the methanol electro-oxidation. This was judged by comparing its higher potential with that of the base state, i.e., Ru(0). The measured methanol electro-oxidation current proves that it is also kinetically more favorable.

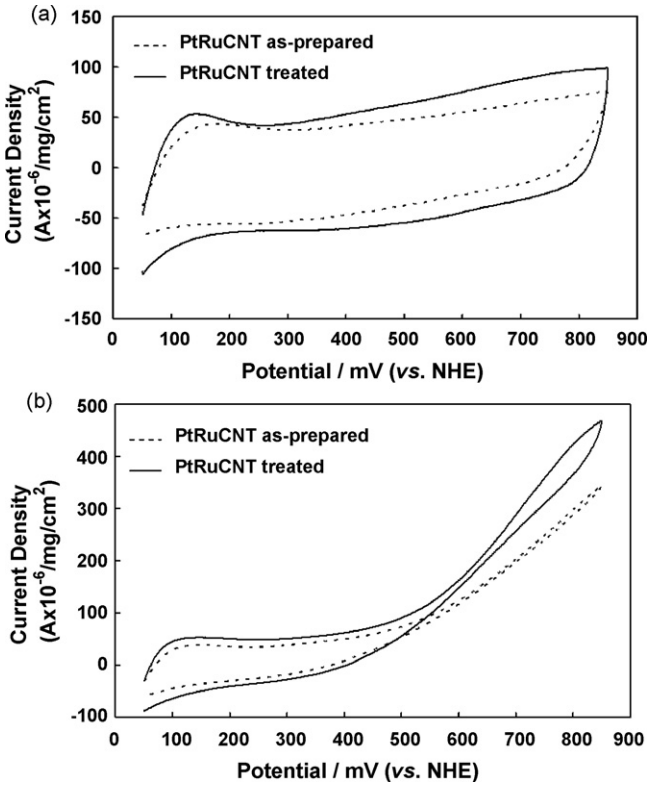

Fig. 7. Cyclic voltammograms of as-prepared (dot line) and treated PtRuCNT (solid line) in (a) 0.5 M H_2SO_4 and (b) 0.5 M H_2SO_4 + 1 M CH_3OH solution at room temperature with a sweep rate of 10 mV s^{-1}.

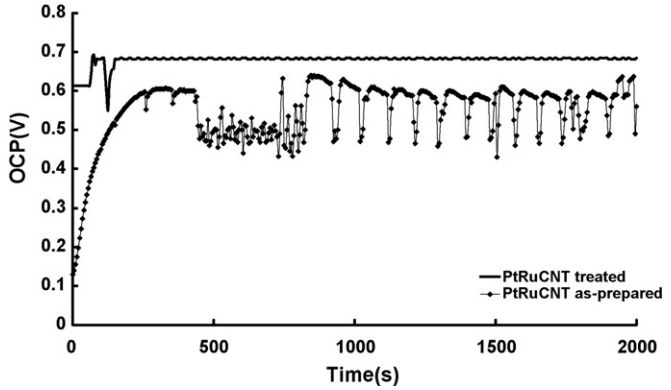

Fig. 8. Open-circuit voltages of a single-cell DMFC incorporated with as-prepared PtRuCNT and treated PtRuCNT catalysts.

In the preparation of electrode, it was found [33] that the catalyst layer containing about 62.3 wt% of dried Nafion® ionomer exhibits the best result. This is quite different from that of an electrode using carbon powder-supported catalyst in which the amount of ionomer is generally much smaller. The high ionomer content was required in this case so as to hold the bulky CNT-supported catalyst well together on the electrode surface.

The open-circuit voltage of a fabricated single-cell DMFC is shown in Fig. 8. It can be seen that the use of a treated PtRuCNT catalyst exhibits a higher voltage than an untreated counterpart, which further demonstrates a more reactive and less resistant anode caused by the increase of the higher oxidation state content of the Ru element. The former also shows a shorter rising time to a steady-state condition. The single-cell test revealed that a direct methanol fuel cell (DMFC) can be run to its full operation in a few minutes. This suggests that a potential application of this finding is to significantly shorten the activation time of a new DMFC stack. The performance of the fabricated single-cell DMFC at 60 °C after having been put into operation for 24 h is illustrated in Fig. 9. It can be seen that the treated catalyst still maintains a better performance in power generation. However, the difference is not very significant. Apparently, the high oxidation state of the ruthenium metal could not be self-regenerated. Most of the Ru(IV) species was eventually converted back to the Ru(0) state in the methanol reaction process. Without a suitable external driving force, there was no reversible mechanism for the Ru(0) species to go back to the Ru(IV) state again. This serious problem has to be resolved for practical applications.

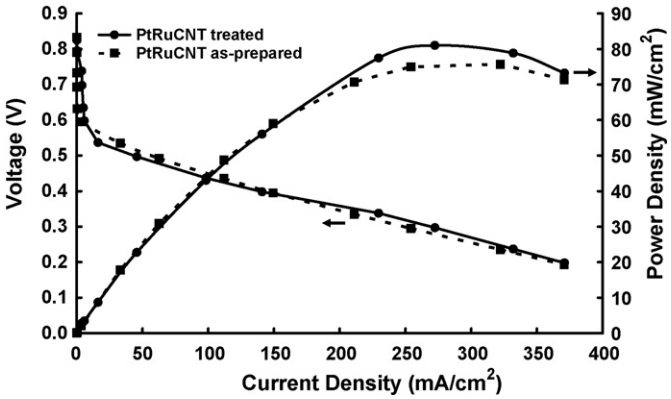

Fig. 9. Performances of a single-cell DMFC incorporated with as-prepared PtRuCNT and treated PtRuCNT catalysts after 24 h into operations at 60 °C.

3.4. Proposed reaction model and suggested solution

So far, the most commonly adopted mechanism to account for the electro-oxidation of methanol on the PtRu catalyst surfaces is the promotional, or bi-functional, mechanism [41,42]. Briefly, in this mechanism the methanol is first dissociated into Pt–$(CO)_{ad}$ and H_{ads} on Pt, while the water is dissociated into Ru–OH and H_{ads} on Ru. Then, Pt–CO_{ad} and Ru–OH react to form CO_2 and H_{ads} eliminating the poisoning effect of CO_{ads} on Pt. Since H_{ad} is an extremely reactive species, it quickly reacts to form H^+ on the catalyst surface. However, the Ru–OH species should be regarded as an energetic intermediate in the reaction process to be meaningful.

Based on the experimental results, a similar promotional reaction model to illustrate the enhanced phenomenon of methanol electro-oxidation is proposed as follows:

$$Pt + CH_3OH \rightarrow Pt{-}(CO)_{ad} + 4H^+ + 4e^- \quad (1)$$

$$RuO_2 + 2Pt{-}(CO)_{ad} \rightarrow Ru + 2Pt + 2CO_2 \quad (2)$$

$$Ru + H_2O \rightarrow Ru{-}OH + H^+ + e^- \quad (3)$$

$$Ru{-}OH + Pt{-}(CO)_{ad} \rightarrow Pt + Ru + CO_2 + H^+ + e^- \quad (4)$$

When the RuO_2 species, i.e., Ru(IV), exists on the catalyst surfaces, the reaction cycle is considered to be composed of Eqs. (1) and (2). After having consumed most of the Ru(IV) species by converting it back to Ru(0), the enhanced PtRuCNT catalyst will become the same as that of a normal catalyst compound. Finally, the Ru–OH species on the catalyst surfaces will have to be generated on the Ru metal as shown in Eq. (3). As a result, the reaction cycle for the methanol electro-oxidation finally will be composed of Eqs. (1), (3) and (4). The Ru(IV) species has a high reduction potential and is obviously more reactive than Ru(0), which needs to be converted to Ru–OH by activation to be useful. This explains the enhancement effect on the methanol electro-oxidation.

It should be noted that although the enhancement of PtRuCNT to its higher oxidation states may not be favorable with respect to electrocatalyst stability, it still deserves more investigations from the viewpoint of catalysis. One of the feasible approaches, perhaps, is to add a small amount of a suitable strong oxidant into the methanol fuel solution continuously or intermittently in a DMFC as a surface oxide-generating additive, which will lead to continuous generation of the RuO_2 species. For instance, hydrogen peroxide (H_2O_2), which has a half-cell reduction potential of 1.776 V and will dissociate into only harmless water and oxygen, is thought to be a good candidate for further investigations. This is based on the perspective of alteration of the oxidation states of catalysts. It was found from our preliminary investigation that the treatment of PtRuCNT by a 3% H_2O_2 solution for 10 min can increase the percentage of the Ru(IV) state to about 40%.

In fact, the use of H_2O_2 as a fuel additive in fuel cells had been reported to be effective on fighting against CO poisoning [43,44]. However, it was simply regarded as a chemical agent used to generate active oxygen to assist the oxidation reaction of CO. Based on our experimental result, this phenomenon should be better to be explained as the ability of H_2O_2 to effectively promote the PtRu catalyst to its higher oxidation states that facilitate the enhanced fuel cell performances.

4. Conclusions

Carbon nanotube-supported PtRu anode catalyst for DMFC applications has been successfully prepared using a modified

polyol method and characterized to have a desired composition and excellent morphology. It was further enhanced using an electrochemical approach to improve the electro-oxidation activity of methanol by modification of the oxidation states of the catalyst elements. From the experimental results, it was identified that the enhanced activity on methanol electro-oxidation mainly came from the substantial increase of the Ru(IV) content from 29.50% to 44.11% in the catalyst. The single-cell DMFC stack could be run at a full operation in a short time. However, the enhanced catalyst needs an extra action to sustain the high activity. A promotional model to explain the reaction of methanol on the PtRu catalyst was proposed. The addition of a suitable oxidant to the fuel to solve the problem encountered is suggested for further investigations.

Acknowledgements

The authors gratefully thank the financial supports from NSTP for Nanoscience and Nanotechnology and Institute of Nuclear Energy Research (INER) of Taiwan for the performance of this work under project number: AEE0302.

References

[1] M. Uchida, Y. Aoyama, N. Tanabe, N. Yanagihara, N. Eda, A. Ohta, J. Electrochem. Soc. 142 (1995) 2572–2576.
[2] E.S. Steigerwalt, G.A. Deluga, C.M. Lukehart, J. Phys. Chem. B 106 (2002) 760–766.
[3] T. Yoshitake, Y. Shimakawa, S. Kuroshima, H. Kimura, T. Icjihashi, Y. Kubo, D. Kasuya, K. Takahashi, F. Kokai, M. Yudasaka, S. Iijima, Physica B 323 (2002) 124–126.
[4] T. Hyeon, S. Han, Y. Sung, K. Park, Y. Kim, Angew. Chem. Int. Ed. 42 (2003) 4352–4356.
[5] R. Yang, X. Qiu, H. Zhang, J. Li, W. Zhu, Z. Wang, X. Huang, L. Chen, Carbon 43 (2005) 11–16.
[6] C.A. Bessel, K. Laubernds, N.M. Rodriguez, R.T.K. Baker, J. Phys. Chem. B 105 (2001) 1115–1118.
[7] J. Guo, G. Sun, Q. Wang, G. Wang, Z. Zhou, S. Tang, L. Jiang, B. Zhou, Q. Xin, Carbon 44 (2006) 152–157.
[8] E.S. Steigerwalt, G.A. Deluga, D.E. Cliffel, C.M. Lukehart, J. Phys. Chem. B 105 (2001) 8079–8101.
[9] K. Park, Y. Sung, S. Han, Y. Yun, T. Hyeon, J. Phys. Chem. B 108 (2004) 939–944.
[10] W. Li, C. Liang, W. Zhou, J. Qiu, H. Li, G. Sun, Q. Xin, Carbon 42 (2004) 436–439.
[11] V. Selvaraj, M. Alagar, K.S. Kumar, App. Catal. B: Environ. 75 (2007) 129–138.
[12] Y. Shao, G. Yin, Y. Gao, P. Shi, J. Electrochem. Soc. 153 (2006) A1093–A1097.
[13] L. Li, Y. Xing, J. Electrochem. Soc. 153 (2006) A1823–A1828.
[14] J. O'M. Bockris, H. Wroblowa, J. Electroanal. Chem. 7 (1964) 428–451.
[15] P. Sivakumar, V. Tricoli, Electrochem. Solid-State Lett. 9 (2006) A167–A170.
[16] J.H. Choi, K.W. Park, I.S. Park, W.H. Nam, Y.E. Sung, Electrochim. Acta 50 (2004) 787–790.
[17] X. Xue, J. Ge, C. Liu, W. Xing, T. Lu, Electrochem. Commun. 8 (2006) 1280–1286.
[18] F. Liu, J.Y. Lee, W. Zhou, J. Electrochem. Soc. 153 (2006) A2133–A2138.
[19] K.W. Park, J.H. Choi, S.A. Lee, C. Park, H. Chang, Y.E. Sung, J. Catal. 224 (2004) 236–242.
[20] A.S. Aricò, Z. Poltarzewski, H. Kim, A. Morana, N. Giordano, V. Antonucci, J. Power Sources 55 (1995) 159–166.
[21] G. Liu, J.S. Cooper, P.J. McGinn, J. Power Sources 161 (2006) 106–114.
[22] M.M.V.M. Souza, N.F.P. Ribeiro, M. Schmal, Int. J. Hydrogen Energy 32 (2007) 425–429.
[23] H. Yano, C. Ono, H. Shiroishi, T. Okada, Chem. Commun. (2005) 1212–1214.
[24] P. Piela, C. Eickes, E. Brosha, F. Garzon, P. Zelenay, J. Electrochem. Soc. 151 (2004) A2053–A2059.
[25] M.K. Jeon, K.R. Lee, K.S. Oh, D.S. Hong, J.Y. Won, S. Li, S.I. Woo, J. Power Sources 158 (2006) 1344–1347.
[26] J.W. Long, R.M. Stroud, K.E. Swider-Lyons, D.R. Rolison, J. Phys. Chem. B 104 (2000) 9772–9776.
[27] A.H.C. Sirk, J.M. Hill, S.K.Y. Kung, V.I. Birss, J. Phys. Chem. B 108 (2004) 689–695.
[28] J. Prabhuram, T.S. Zhao, Z.X. Liang, R. Chen, Electrochim. Acta 52 (2007) 2649–2656.
[29] Y. Liang, H. Zhang, H. Zhong, X. Zhu, Z. Tian, D. Xu, B. Yi, J. Catal. 238 (2006) 468–476.
[30] Z. Liu, J.Y. Lee, W. Chen, M. Han, L.M. Gan, Langmuir 20 (2004) 181–187.
[31] C.C. Chien, K.T. Jeng, Mater. Chem. Phys. 99 (2006) 80–87.
[32] K.T. Jeng, C.C. Chien, N.Y. Hsu, S.C. Yen, S.D. Chiou, S.H. Lin, W.M. Huang, J. Power Sources 160 (2006) 97–104.
[33] K.T. Jeng, C.C. Chien, N.Y. Hsu, W.M. Huang, S.D. Chiou, S.H. Lin, J. Power Sources 164 (2007) 33–41.
[34] Y. Takasu, T. Kawaguchi, W. Sugimoto, Y. Murakami, Electrochim. Acta 48 (2003) 3861–3868.
[35] A.S. Aricò, P.L. Antonucci, E. Modica, V. Baglio, H. Kim, V. Antonucci, Electrochim. Acta 47 (2002) 3723–3732.
[36] V. Radmilovic, H.A. Gasteiger, P.N. Ross Jr., J. Catal. 154 (1995) 98–106.
[37] C.C. Chien, K.T. Jeng, Mater. Chem. Phys. 103 (2007) 400–406.
[38] M. Pourbaix, Atlas of Electrochemical Equilibrium in Aqueous Solutions, NACE International, Houston, 1974, pp. 343–383.
[39] M.-S. Hynn, S.-K. Kim, B. Lee, D. Peck, Y. Shul, D. Jung, Catal. Today 132 (2008) 138–145.
[40] M.V. Martínez-Huerta, S. Rojas, J.L. Gómez de la Fuente, P. Terreros, M.A. Pena, J.L.G. Fierro, App. Catal. B: Environ. 69 (2006) 75–84.
[41] M. Watanabe, S. Motoo, J. Electroanal. Chem. 60 (1975) 267–273.
[42] C. Bock, M.A. Blakely, B. MacDougall, Electrochim. Acta 50 (2005) 2401–2414.
[43] V.M. Schmidt, H.-F. Oetjen, J. Divisek, J. Electrochem. Soc. 144 (1997) L237–L238.
[44] J. Divisek, H.-F. Oetjen, V. Peinecke, V.M. Schmidt, U. Stimming, Electrochim Acta 43 (1998) 3811–3815.